

Tetragonal and Helical Morphologies from Polyferrocenylsilane Block Polyelectrolytes via Ionic Self-Assembly

Rumman Ahmed,[†] Sanjib K. Patra,^{†,§} Ian W. Hamley,[‡] Ian Manners,^{*,†} and Charl F. J. Faul^{*,†}

[†]School of Chemistry, University of Bristol, Cantock's Close, Bristol BS8 1TS, U.K.

[‡]Department of Chemistry, University of Reading, Whiteknights, P.O. Box 217, Reading, Berkshire RG6 6AH, U.K.

S Supporting Information

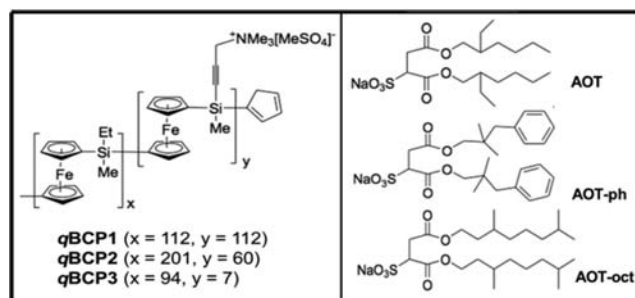
ABSTRACT: The use of ionic self-assembly, a facile non-covalent approach, to access non-conventional block copolymer morphologies, including tetragonal and helical structures, from a combination of polyferrocenylsilane diblock copolymer polyelectrolytes and AOT-based surfactants, is described.

Block copolymers (BCPs) are attracting growing interest as the incompatibility between chemically different blocks that are linked together enables phase-separation to take place on the nanoscale.^{1,2} This versatile approach can be utilized to access a series of well-ordered arrays of nanometer-sized domains.³ In AB diblock copolymers, the well-studied thermodynamically stable solid-state morphologies include spherical, cylindrical, gyroid, and lamellar structures, with their formation mainly depending on the relative volume fractions (Φ) of the segments.^{2c,4} The generation of other more complex morphologies is of major current interest to further expand the range of available applications of BCPs.^{1,3a} For example, square arrays⁵ are desirable for information storage applications, and convenient access was recently achieved by the combination of supramolecular hydrogen-bonding interactions with diblock copolymer self-assembly.⁶ Other methods reliant on non-covalent interactions to fabricate complex, self-organized supramolecular materials from BCPs have utilized crystallization,⁷ π -stacking,⁸ and ionic and hydrophobic interactions.⁹

We have exploited the use of electrostatic interactions inherent to the ionic self-assembly (ISA) approach to produce polymeric supramolecules, in which polymer and surfactant self-assembly and physical properties are favorably combined.¹⁰ The use of block polyelectrolytes (i.e., BCPs in which at least one block is ionically charged) for the ISA strategy has led to intricate hierarchical comb-coil BCP structures,¹¹ porous organic woodpile assemblies,¹² and double smectic-like self-assemblies in the solid-state,¹³ thereby illustrating the ability to induce periodic order at different length scales. In order to explore additional complex behavior and to introduce orthogonally addressable polymer functions to ISA materials, we have recently explored the use of metal-containing polyferrocenylsilane (PFS) polyelectrolytes and block polyelectrolytes as ISA components.¹⁴ These materials are attractive as they combine the properties of PFS (such as redox-activity,¹⁵ etch-resistance,¹⁶ and ability to function as a magnetic¹⁷ and catalytically active ceramic precursor¹⁸) with the processability

of polyelectrolytes. In this Communication we report our preliminary results concerning the formation of, and control over, hierarchically structured ISA materials using all-PFS diblock co-polyelectrolytes (Chart 1). We show that BCP phase

Chart 1. ISA Complexations of the Block Polyelectrolytes with the AOT-Based Surfactants



morphologies can be adjusted by tuning of the respective block volume fractions and by surfactant addition. Most significantly, we demonstrate that the use of this strategy allows access to non-classical morphologies on the phase diagram for diblock copolymers.

The PFS diblock polyelectrolytes utilized in this study were prepared via sequential photolytic ring-opening polymerization of strained sila[1]ferrocenophanes followed by quaternization of the amino groups present in one block (see Supporting Information, Scheme S1). This living polymerization method allowed the preparation of PFS block polyelectrolyte precursors, poly(ferrocenylethylmethylsilane)-*block*-poly(ferrocenylmethyl(dimethylaminopropynyl)silane)s (PFEMS-*b*-PFAMS), with different block ratios, well-controlled molecular weights, and narrow molecular weight distributions (<1.1 , Figure S1).¹⁹ The three diblock copolymers studied here exhibited similar thermal characteristics (see e.g. Figure S2). Quaternization of the diblock copolymers in THF/methanol using dimethyl sulfate^{19b} resulted in the corresponding block polyelectrolytes $qBCP1$ - $qBCP3$ (Chart 1). These materials were characterized by ¹H NMR spectroscopy (in *d*₈-THF, see Figure S3 and Table S1 for a summary).

Following quaternization, a selection of surfactant species was used in the ISA approach: the AOT family of surfactants shown in Chart 1 was chosen to provide benchmark

Received: December 17, 2012

Published: January 22, 2013

complexations to investigate the effect of aryl groups (AOT-ph) and of further alkyl branching (AOT-oct) on the final supramolecular architectures. The selective loading of low-molecular-weight amphiphiles to the PFAMS block increased its volume fraction, resulting in an overall (expected) phase change at the BCP length scale (e.g., phase changes between lamellae and cylinders were observed).

The complexation of *q*BCP1 with AOT, AOT-ph, and AOT-oct yielded *cylinder-within-lamellar* morphologies (Figure S5 and Scheme S2a) on the BCP length scale, and, on the surfactant length scale, a lamellar pattern was observed as a result of the surfactant alkyl tail interdigitation. However, the differences in the surfactant tail topology between AOT, AOT-ph, and AOT-oct had minimum influence on the overall morphology, which in each case was cylindrical (see Scheme S2a for a summary). In contrast, both of the ISA complexes with *q*BCP2, *q*BCP2-AOT and *q*BCP2-AOT-ph, yielded the expected *lamellar-within-lamellar* morphologies (see Scheme S2b for an illustrative example of the hierarchical self-assembly, and Figures S6 and S7 for detailed characterization of the *q*BCP2-AOT and *q*BCP2-AOT-ph complexes, respectively). Small-angle X-ray scattering (SAXS) reflections at the larger length scale were consistent with a lamellar morphology, with an average *d*-spacing of 33 nm for *q*BCP2-AOT-ph (reflections in the ratios of 1:2:3:4:5 were observed). SAXS reflections at the smaller length scale also corresponded to a lamellar morphology, with an average *d*-spacing of 2.2 nm (reflections in the ratio of 1:2), as seen in Figures S6b, inset, and S7d. 2D SAXS data showed the presence of ordered anisotropic material, which strongly suggests the presence of π -interactions playing a role in nanodomain alignment over larger length scales. This was further supported by transmission electron microscopy (TEM) analysis (Figures S6c and S7b), where the hierarchically ordered domains were aligned over several micrometers.

Unlike the other complexes with *q*BCP2, *q*BCP2-AOT-oct yielded a *tetragon-within-lamellar* morphology. SAXS reflections at low *q* regions are indicative of a tetragonal morphology with a *d*-spacing of 36 nm (Figure 1a). These data were complemented by bright-field TEM analysis, which clearly showed ordered square-packing arrangements across several micrometers (Figure 1b), with the lighter matrix corresponding to the PFAMS-AOT-oct block, and the darker squares consistent with the PFEMS block. Energy-dispersive X-ray (EDX) analysis of the tetragons and the matrix confirmed the presence of the amphiphile (clearly indicated by the presence of sulfur atoms originating from the surfactant head group) within the matrix (Figure 1c,d). Furthermore, the SAXS reflections observed at the surfactant length scale (Figure 1a, inset) showed a lamellar ordering with a *d*-spacing of 3.0 nm.

In addition, birefringent textures were observed under crossed polarizers during polarized optical microscopy investigations, indicative of optically anisotropic materials, thus ruling out the presence of a “classical” optically isotropic cubic phase (Figure S8a). We therefore conclude that the hierarchical self-assembly of the comb-coil diblock-surfactant complex has generated tetragonally packed PFEMS columns embedded in the lamellar mesophase of the PFAMS-AOT-oct block. The volume and architecture of the alkyl tail played a key role in the formation of this unforeseen morphology. This finding is noteworthy, as the complexation of *q*BCP2 with both AOT and AOT-ph gave the expected *lamellar-within-lamellar* morphologies. The only difference for AOT-oct was the

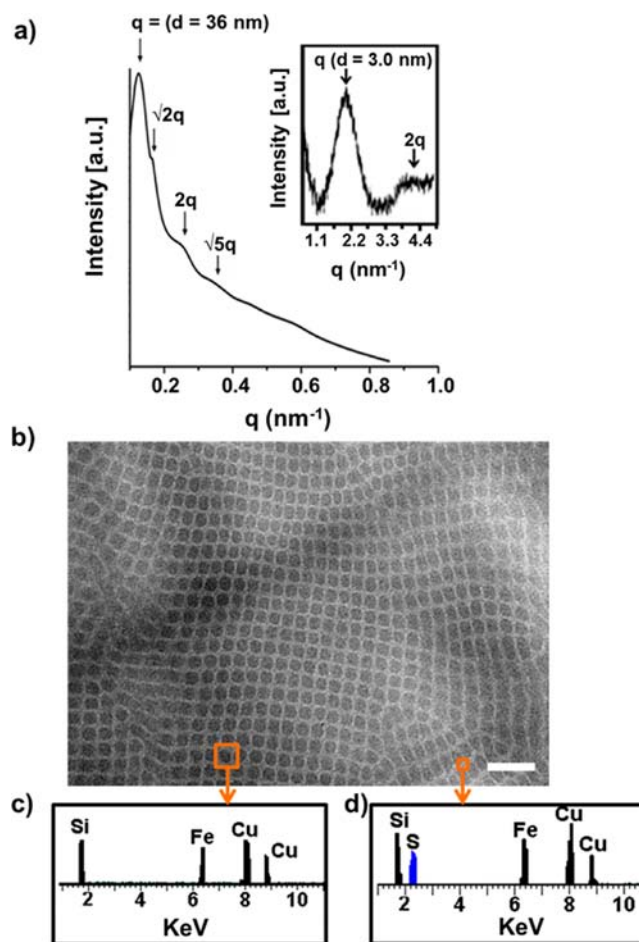


Figure 1. Characterizations of *q*BCP2-AOT-oct: (a) SAXS showing a square packing morphology at the larger length scale; inset, SAXS at the smaller length scale; (b) TEM micrograph (scale bar = 200 nm); (c) EDX analysis of the dark squares; (d) EDX analysis of the lighter matrix.

architecture and volume of the alkyl tails, with the tail volumes increasing from 0.39 (AOT) and 0.50 (AOT-ph) to 0.57 nm³ in AOT-oct.²⁰

In our particular case, we believe conformational restrictions occur due to the presence of octyl groups ionically bound to the PFAMS block, which produces a “bottle brush” structure. Presumably, this gives rise to a greater asymmetry between the blocks, resulting in significant incommensurability and packing constraints and consequent chain stretching for the PFAMS block. These constraints then cause the morphology to shift from the expected lamellar to the observed tetragonal arrangement. The approach here is similar to studies where a “conformational asymmetry” parameter (ζ) was introduced to allow for differences in space-filling of different blocks.²¹ The main effect of ζ is to shift the phase boundaries toward compositions richer in the segments with the higher asymmetry. To date, only limited examples of such morphologies from diblock copolymers or AB/B’C diblock copolymer blends with hydrogen-bonding interactions have been observed.^{6,22}

Surfactant complexation of *q*BCP3 and AOT was expected to lead to the formation of a cylindrical morphology (theoretical predictions and calculations of volume fractions showed an increase from Φ_{PFAMS} 0.1 to 0.3). However, TEM analysis showed the presence of lighter helical twists within a

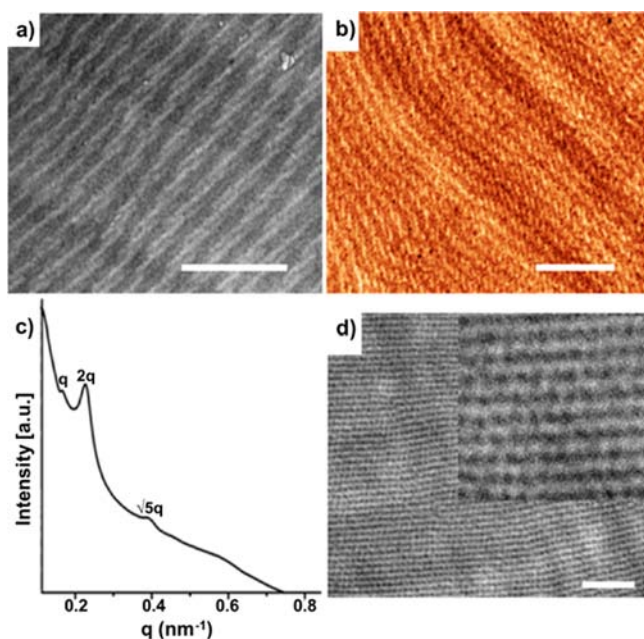


Figure 2. Morphological characterization of q BCP3-AOT: (a) TEM showing helices (scale bar = 200 nm); (b) helices as shown by imaging of the TEM grid by tapping-mode AFM (scale bar = 500 nm); (c) SAXS pattern showing tetragonal packing at larger length scales; (d) tetragonal packing by TEM (scale bar = 1000 nm).

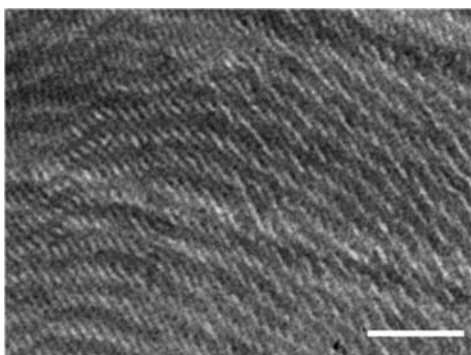


Figure 3. TEM micrograph of large-area helical structures from q BCP3-AOT-oct (scale bar = 200 nm).

darker matrix (Figure 2a), indicating the presence of a helical morphology. The average pitch of these helical structures was calculated to be 18 nm. In addition, direct imaging of the TEM grid using tapping-mode atomic force microscopy (AFM) provided further evidence of the helical structures (Figure 2b). Other regions of the grid (Figure 2d) showed tetragonal packing of the hierarchical system similar to that seen for q BCP2-AOT-oct. Furthermore, SAXS reflections (Figure 2c) at q ratios of $1:\sqrt{4}:\sqrt{5}$ confirmed tetragonal packing, which fitted well with the data (as the preferential arrangement of the helices can be in a tetragonal manner). Lastly, these materials also displayed highly birefringent textures (Figure S8b).

To ascertain whether this helical morphology was specific to the AOT surfactant alone, q BCP3-AOT-oct and q BCP3-AOT-ph were also prepared. TEM results in both cases indicated the presence of helices (see Figure 3 for a representative example). EDX studies showed that the lighter, surfactant-containing parts form the helical motif (Figure S9).

In summary, we have shown that ionic self-assembly of polyferrocenylsilane block polyelectrolytes with low-molecular-weight amphiphiles based on the common surfactant, AOT, provides a simple route to construct intricate morphologies not predicted by conventional linear AB block copolymer phase diagrams. Further studies aim to establish the general applicability of this approach to access morphologies of technological interest. For example, the etch-selectivity of PFS makes thin films of these materials interesting candidates for nanolithographic applications.

■ ASSOCIATED CONTENT

📄 Supporting Information

Details of synthesis and characterization. This material is available free of charge via the Internet at <http://pubs.acs.org>.

■ AUTHOR INFORMATION

Corresponding Author

ian.manners@bristol.ac.uk; charl.faul@bristol.ac.uk

Present Address

[§]Department of Chemistry, Indian Institute of Technology, Kharagpur 721302, India

Notes

The authors declare no competing financial interest.

■ ACKNOWLEDGMENTS

C.F.J.F. thanks the University of Bristol for financial support. S.K.P. thanks the EU for a Marie Curie Postdoctoral Fellowship, and I.M. thanks EPSRC for support.

■ REFERENCES

- (1) (a) Lodge, T. P. *Macromol. Chem. Phys.* **2003**, *204*, 265. (b) Hadjichristidis, N.; Pitsikalis, M.; Pispas, S.; Iatrou, H. *Chem. Rev.* **2001**, *101*, 3747. (c) Hamley, I. W. *Angew. Chem., Int. Ed.* **2003**, *42*, 1692. (d) Schacher, F. H.; Rupar, P. A.; Manners, I. *Angew. Chem., Int. Ed.* **2012**, *51*, 7898.
- (2) (a) Darling, S. B. *Prog. Polym. Sci.* **2007**, *32*, 1152. (b) Krausch, G.; Magerle, R. *Adv. Mater.* **2002**, *14*, 1579. (c) Hamley, I. W. *The Physics of Block Copolymers*; Oxford Science Publications: Oxford, 1998.
- (3) (a) Bates, F. S.; Fredrickson, G. H. *Phys. Today* **1999**, *52*, 32. (b) Lodge, T. P.; Muthukumar, M. J. *Phys. Chem.* **1996**, *100*, 13275. (c) Khandpur, A. K.; Förster, S.; Bates, F. S.; Hamley, I. W.; Ryan, A. J.; Bras, W.; Almdal, K.; Mortensen, K. *Macromolecules* **1995**, *28*, 8796.
- (4) Matsen, M. W.; Bates, F. S. *Macromolecules* **1996**, *29*, 1091.
- (5) Chuang, V. P.; Gwyther, J.; Mickiewicz, R. A.; Manners, I.; Ross, C. A. *Nano Lett.* **2009**, *9*, 4364.
- (6) Tang, C.; Lennon, E. M.; Fredrickson, G. H.; Kramer, E. J.; Hawker, C. J. *Science* **2008**, *322*, 429.
- (7) Rupar, P. A.; Chabanne, L.; Winnik, M. A.; Manners, I. *Science* **2012**, *337*, 559.
- (8) Thünemann, A. F.; Kubowicz, S.; Burger, C.; Watson, M. D.; Tchebotareva, N.; Müllen, K. *J. Am. Chem. Soc.* **2003**, *125*, 352.
- (9) (a) Hammond, M. R.; Mezzenga, R. *Soft Matter* **2008**, *4*, 952. (b) Ikkala, O.; ten Brinke, G. *Chem. Commun.* **2004**, 2131.
- (10) (a) Zhang, T. R.; Brown, J.; Oakley, R. J.; Faul, C. F. J. *Curr. Opin. Colloid Interface Sci.* **2009**, *14*, 62. (b) Faul, C. F. J.; Antonietti, M. *Adv. Mater.* **2003**, *15*, 673.
- (11) (a) Houbenov, N.; Haataja, J. S.; Iatrou, H.; Hadjichristidis, N.; Ruokolainen, J.; Faul, C. F. J.; Ikkala, O. *Angew. Chem., Int. Ed.* **2011**, *50*, 2516. (b) Houbenov, N.; Nykänen, A.; Iatrou, H.; Hadjichristidis, N.; Ruokolainen, J.; Faul, C. F. J.; Ikkala, O. *Adv. Funct. Mater.* **2008**, *18*, 2041.

(12) Toombes, G.; Mahajan, S.; Weyland, M.; Jain, A.; Du, P.; Kamperman, M.; Gruner, S.; Muller, D.; Wiesner, U. *Macromolecules* **2008**, *41*, 852.

(13) Haataja, J. S.; Houbenov, N.; Iatrou, H.; Hadjichristidis, N.; Karatzas, A.; Faul, C. F. J.; Rannou, P.; Ikkala, O. *Biomacromolecules* **2012**, *13*, 3572.

(14) (a) Ahmed, R.; Hsiao, M.-S.; Matsuura, Y.; Houbenov, N.; Faul, C. F. J.; Manners, I. *Soft Matter* **2011**, *7*, 10462. (b) Ahmed, R.; Patra, S. K.; Chabanne, L.; Faul, C. F. J.; Manners, I. *Macromolecules* **2011**, *44*, 9324. (c) Ma, V. Y.; Dong, W. F.; Hempenius, M. A.; Möhwald, H.; Vancso, G. J. *Angew. Chem., Int. Ed.* **2007**, *46*, 1702. (d) Ahmed, R.; Priimagi, A.; Faul, C. F. J.; Manners, I. *Adv. Mater.* **2012**, *24*, 926. (e) Cheng, Z. Y.; Ren, B. Y.; Zhao, D. L.; Liu, X. X.; Tong, Z. *Macromolecules* **2009**, *42*, 2762.

(15) (a) Ma, V. Y.; Dong, W. F.; Hempenius, M. A.; Möhwald, H.; Vancso, G. J. *Nat. Mater.* **2006**, *5*, 724. (b) Eitouni, H. B.; Balsara, N. P. *J. Am. Chem. Soc.* **2004**, *126*, 7446. (c) Eloi, J. C.; Rider, D. A.; Cambridge, G.; Whittell, G. R.; Winnik, M. A.; Manners, I. *J. Am. Chem. Soc.* **2011**, *133*, 8903. (d) Puzzo, D. P.; Arsenault, A. C.; Manners, I.; Ozin, G. A. *Angew. Chem., Int. Ed.* **2009**, *48*, 943. (e) Shi, W.; Giannotti, M. I.; Zhang, X.; Hempenius, M. A.; Schönherr, H.; Vancso, G. J. *Angew. Chem., Int. Ed.* **2007**, *46*, 4800.

(16) (a) Chuang, V. P.; Ross, C. A.; Gwyther, J.; Manners, I. *Adv. Mater.* **2009**, *21*, 3789. (b) Acikgoz, C.; Ling, X. Y.; Phang, I. Y.; Hempenius, M. A.; Reinhoudt, D. N.; Huskens, J.; Vancso, G. J. *Adv. Mater.* **2009**, *21*, 2064. (c) Korczagin, I.; Lammertink, R. G. H.; Hempenius, M. A.; Golze, S.; Vancso, G. J. *Adv. Polym. Sci.* **2006**, *200*, 91. (d) Lu, J.; Chamberlin, D.; Rider, D. A.; Liu, M.; Manners, I.; Russell, T. P. *Nanotechnology* **2006**, *17*, 5792.

(17) Rider, D. A.; Eloi, J. C.; Liu, K.; Eloi, J. C.; Vanderark, L.; Yang, L.; Wang, J. Y.; Grozea, D.; Lu, Z. H.; Manners, I.; Russell, T. P. *ACS Nano* **2008**, *2*, 263.

(18) (a) Hinderling, C.; Keles, Y.; Stockli, T.; Knapp, H. E.; de los Arcos, T.; Oelhafen, P.; Korczagin, I.; Hempenius, M. A.; Vancso, G. J.; Pugin, R. L.; Heinzlmann, H. *Adv. Mater.* **2004**, *16*, 876. (b) Lastella, S.; Jung, Y. J.; Yang, H. C.; Vajtai, R.; Ajayan, P. M.; Ryu, C. Y.; Rider, D. A.; Manners, I. *J. Mater. Chem.* **2004**, *14*, 1791.

(19) (a) Tanabe, M.; Vandermeulen, G. W. M.; Chan, W. Y.; Cyr, P. W.; Vanderark, L.; Rider, D. A.; Manners, I. *Nat. Mater.* **2006**, *5*, 467. (b) Wang, Z.; Masson, G.; Peiris, F. C.; Ozin, G. A.; Manners, I. *Chem. Eur. J.* **2007**, *13*, 9372. (c) Herbert, D. E.; Gilroy, J. B.; Chan, W. Y.; Chabanne, L.; Staubitz, A.; Lough, A. J.; Manners, I. *J. Am. Chem. Soc.* **2009**, *131*, 14958.

(20) Krevelen, D. W. v. *Properties of Polymers*, 3rd ed.; Elsevier: Amsterdam, 1990.

(21) (a) Vavasour, J. D.; Whitmore, M. D. *Macromolecules* **1993**, *26*, 7070. (b) Bates, F. S.; Fredrickson, G. H. *Macromolecules* **1994**, *27*, 1065.

(22) Chen, H. L.; Lu, J. S.; Yu, C. H.; Yeh, C. L.; Jeng, U. S.; Chen, W. C. *Macromolecules* **2007**, *40*, 3271.